**Title**
The cross-aisle seismic performance of storage rack base connections



**Authors**
Petrone, F
Higgins, PS
Bissonnette, NP
et al.

**Publication Date**
2016-07-01

**DOI**
10.1016/j.jcsr.2016.04.014

Peer reviewed

Journal of Constructional Steel Research 122 (2016) 520–531

Contents lists available at ScienceDirect

Journal of Constructional Steel Research

# The cross-aisle seismic performance of storage rack base connections

F. Petrone [a], P.S. Higgins [b], N.P. Bissonnette [c], A.M. Kanvinde [d,*]

[a] Lawrence Berkeley National Laboratory, Earth Science Division, Berkeley, CA, USA
[b] Peter S Higgins and Associates, USA
[c] Frazier Industrial Company, Long Valley, NJ, USA
[d] Department of Civil and Environmental Engineering, University of California, Davis, CA, USA

ARTICLE INFO

*Article history:*
Received 28 October 2015
Received in revised form 6 April 2016
Accepted 13 April 2016

*Keywords:*
Seismic response
Storage racks
Base connections
Finite element simulation

ABSTRACT

Steel storage racks used in retail stores and warehouses are seismically designed as moment resisting frames in the down-aisle direction, and braced frames in the cross-aisle direction. While their down-aisle response is relatively well understood, there is little understanding of their cross-aisle response, especially as it pertains to the desired mode of inelastic deformation and associated design methods. Results are presented from six full scale tests on braced frames representing storage racks in the cross-aisle direction. These tests investigate the base plate thickness and dimensions, and the upright (column) cross section. The experiments indicate that inelastic deformation in the base plate provides stable hysteretic response with significant ductility and energy dissipation. Ductile tearing is also observed in welds connecting the base plate to the upright. However, it does not appear to negatively influence the hysteretic response. The tests are complemented by Finite Element (FE) simulations of the base connections. These simulations provide insights into internal force distributions within the connections. Based on these insights, analytical equations are proposed for characterizing the backbone curve of the hysteretic response, for use in displacement based design methods. It is determined that the current approach for characterizing design forces in the anchors is unconservative, since it does not incorporate the effects of strain hardening or the membrane action as the base plate undergoes large deformations. A new approach which incorporates these phenomena is presented, and determined to be significantly more accurate. Limitations of the study are outlined and directions for future work are identified.



## 1. Introduction

Steel storage racks are commonly used in facilities such as warehouses and "big-box" retail stores. Shown in Fig. 1a, these racks are typically 8–30 ft tall, although racks exceeding 100 ft high are not uncommon, and support heavy loads (often 30–50 times their self-weight). The structural performance of these racks has obvious implications for structural safety, since collapse (due to overturning in the cross-aisle direction) has the potential of causing serious injury or fatality. This type of collapse has been documented in prior earthquakes, most notably in retail stores in Santa Clarita, California, and Canoga Park, California, during the 1994 Northridge earthquake; see Fig. 1b, adapted from FEMA 460 [1]. While the result of overloading, these failures demonstrate the potential for personnel danger and property loss. More recently, some damage to racks (element buckling) was also observed during the smaller 2001 Nisqually, Washington earthquake.

Referring to Fig. 1a, the racks are configured as moment-resisting frames in the down-aisle direction (parallel to the shopping aisle), to facilitate placing and removal of inventory. In the cross-aisle direction, the racks are configured as braced frames. In this direction, the racks are narrow and more susceptible to overturning, as compared to the down-aisle direction, where the main issue is sidesway collapse. Several studies have investigated the response of storage racks. These include quasi static tests by Krawinkler et al., [2], Higgins [3], and Bernuzzi and Castiglioni [4], as well as dynamic tests by Blume [5], Chen et al., [6], Castiglioni et al., [7], and more recently by Filiatrault and Higgins [8], and Filiatrault and Wanitkorkul [9]. These studies have been complemented by analytical and numerical studies, e.g., by Coutinho [10], cumulatively resulting in design practices for storage racks; FEMA 460 [1] outlines these practices in detail. Referring to FEMA 460 [1] and these studies, it is noted that –

1. A majority of the studies has focused on the down-aisle response, and associated design practices. As a result, the understanding of cross-aisle response is limited, and unlike the down-aisle (moment frame) response in which the beams yield, the ductile/dissipative mechanism in the cross-aisle direction is not as well defined. In fact, the shake table tests by Chen et al. [11] indicate that inelastic deformations in the cross-aisle directions are highly localized (in the connection region between the bracing elements and the uprights).

* Corresponding author.
*E-mail address:* kanvinde@ucdavis.edu (A.M. Kanvinde).

http://dx.doi.org/10.1016/j.jcsr.2016.04.014
0143-974X/

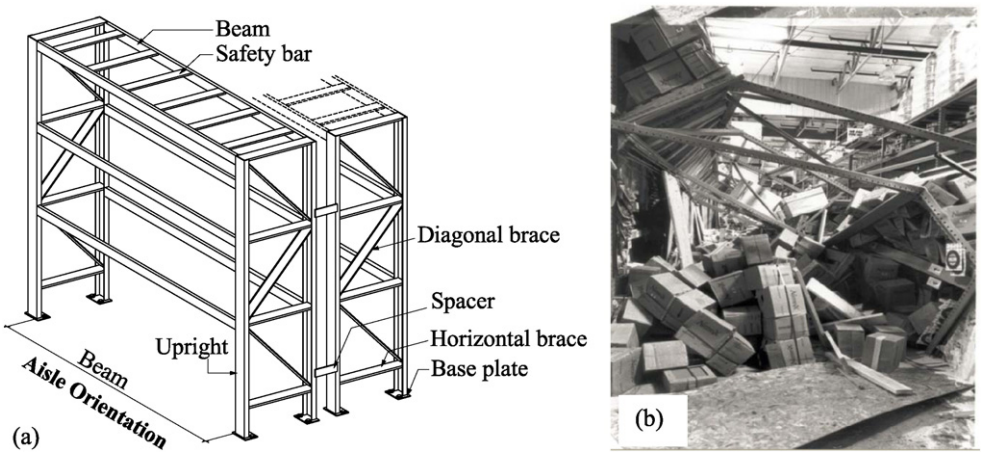


**Fig. 1.** (a) Schematic illustration of rack system (b) collapse in Santa Clarita store.

Consequently, the overall dissipative/inelastic response of the system in the cross-aisle direction is minimal. On the other hand, the studies indicate that the down-aisle response is highly ductile, with story drifts as large as 7% before incipient collapse [6].

2. The methods currently used for the design of these racks are force-based, i.e., they rely on an equivalent lateral load, which is calculated through a strength reduction (or R) factor. Typically, the R factor is taken as 6.0 in the down-aisle direction, and 4.0 in the cross aisle direction.
3. While commonly used for design, the current R factors are empirical. They arise (as working stress values) from Standard 27-11 of the 1975 Uniform Building Code [12], and have survived with little change (aside from conversion to LRFD equivalents) in RMI/ANSI MH16.1 [13], the rack design standard incorporated into ASCE-7 [14]. The ASCE-7 code accepts the R values of ANSI MH16.1 [13], but has increased the demands for anchorage in section 15.5.3. While [13] outlines Displacement Based Design (DBD) criteria in both directions, it is primarily used in the down aisle direction. This is a result of the extensive testing done over many years (e.g., [6–8]) to characterize this response. A design method for the down-aisle direction is suggested in FEMA 460 [1]. While the DBD fundamentals apply equally to both directions, at the time of writing FEMA 460, little data was available for response in the cross-aisle direction. Accordingly, a design method was not proposed.

Motivated by these issues, the main objectives of this study are the following:

1. To examine through quasi-static tests, and finite element simulations, the potential for using base connection yielding accompanied by frame rocking as a dissipative mechanism for the seismic response of racks in the cross-aisle direction. Previous experimental studies by Midorikawa et al. [15] and Huckleridge [16] have demonstrated the feasibility of rocking structural systems with energy dissipation in the base connection. More recently, full-scale shake table tests by Ma et al. [17] and analytical studies by Acikgoz et al. [18] have confirmed this to be an attractive mechanism for dissipating seismic energy and controlling the risk of excessive deformations or collapse. However, being focused on building systems, these have not specifically considered base connections in storage racks (which are constrained in terms of size and layout), or their inelastic response within the overall dynamic response of the structure. Fig. 2 schematically illustrates a typical base connection in a storage rack, indicating that it is subjected to predominantly one-dimensional (vertical) cyclic loading as the frame undergoes lateral motions and rocking in the cross-aisle direction.
2. To develop a framework for characterizing the load-deformation response of base connections when subjected to cross-aisle loading, with two aims: (1) to provide an aid for displacement-based design of racks when the base-yielding mechanism is desired (2) to provide a framework for simulation of cross-aisle response, ultimately supporting parametric simulation for development of generalized design guidelines.
3. To provide guidelines for the design and detailing of the bases themselves. Referring to Fig. 2, the base connections consist of the upright (the column, which is typically a box or a channel section) welded to a base plate, which in turn is anchored to the concrete floor using post-installed anchors. Yielding of the base plate is the preferred mode of inelastic dissipation. As a result, from a connection design perspective, two issues are relevant: (1) detailing of the base plate, including size, thickness, and weld details to ensure ductile response under expected deformation demands, and (2) estimation of design forces in the anchors to withstand the demands imposed by the yielding base plate. The latter is critical, since post-installed anchors (which are the most common method of connecting the base plate to the warehouse floor) are brittle (Gesoglu et al. [19]), and consequently must be designed using capacity design principles. Moreover, the response of the base plate itself is controlled by material hardening, geometric nonlinearity due to the membrane action of the plate as the deformations increase, and phenomena such as contact and prying. These phenomena warrant consideration in any method to compute design forces in the anchor rods.

The main scientific basis of this study is a series of 6 quasi-static experiments, and complementary Finite Element (FE) simulations of base connections in storage racks. The experiments feature braced

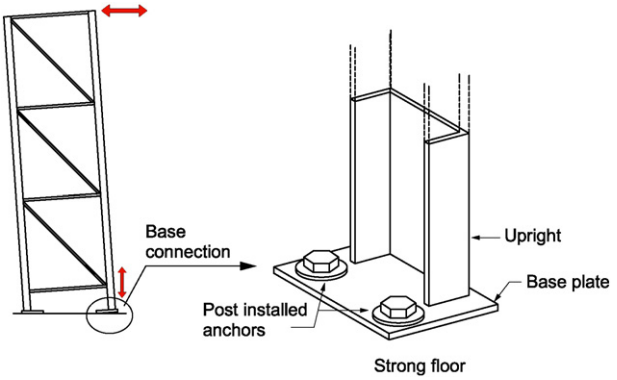


**Fig. 2.** Schematic illustration of frame response mode and base connection.

frames similar to those used in racks in the cross-aisle direction, and base connections with a weak (yielding) base plate. The experiments provide an examination of the weak-base concept, as well as validation of the simulations. The simulations provide physical insight into the internal force distributions and deformation patterns in a manner (and at a resolution) that the experiments cannot; these insights may be used to idealize the physical response, and eventually develop analytical models for load-deformation as well as design of the anchors. The paper begins by outlining the findings of the experiments, and data that is used for validation and model development. The subsequent section discusses the FE simulations themselves. This is followed by a presentation of the analytical models based on the FE simulations. The paper concludes by summarizing the findings, design considerations, and limitations.

## 2. Experimental study—setup, instrumentation, and results

Fig. 3a schematically illustrates the full-scale braced frame, such that in-plane lateral forces represent cross-aisle loading of the racks. Table 1 summarizes the test matrix. Referring to the Table, the main variables investigated include: (1) plate layout, i.e., plan dimensions, (2) plate thickness, and (3) upright size and shape, which included channels and built up box sections constructed from two channels. The frames are designed such that all inelastic action is concentrated in the base connection, which undergoes cyclic motions in the (predominantly) vertical direction. Fig. 3b shows the elevation view of a generic base connection detail, to indicate some of the dimensional quantities, as well as the instrumentation provided at the base.

Fig. 4a–d show the various plan dimensions listed in Table 1; all of these may be associated with the generic elevation view shown in Fig. 3b. Some of these experiments, e.g., 4, and 5, 6 reflect those used in design practice, whereas some (1, 2 and 3) feature alternate configurations (for example low thickness in Tests #1 and #3, and an extended plate toe, i.e., the dimension $n = 3.5$ in. for the plate toe in both Tests #1, and #2 with layout A) to explore the possibility of improved performance. Other features of the experiments are now summarized:

1. The overall dimensions of the frame (i.e., h = 118 in. and b = 35 in.) were similar for all the specimens. For the box section configuration, the uprights were different only in the base region, for a height of 12 in. in plan layout C and 44 in. in plan layout D.
2. The specimens were loaded laterally by an actuator attached to the top as shown in Fig. 3a. The loading was applied in displacement control similar to the ATC-24 [20] protocol. It is important to emphasize that these tests are intended to represent component hysteretic response, and consequently the displacement controlled loading is appropriate. More specifically, the frame does not include gravity loads, since in the context of this test program, such loads would only alter the relationship between the applied lateral load and upright force, without materially influencing the hysteretic response of the connection itself.
3. All the uprights were connected to the base plates through 0.1875 in. fillet welds. For the box sections, these welds were deposited from the outside. For the channel sections, the welds were deposited from the outside of the web, and from inside edge of one flange, and outside edge of the other. The welds are schematically illustrated in Fig. 4a–d.
4. Referring to Fig. 3b, the frame was affixed to a 4 in. thick steel plate which formed the reaction system (similar to a strong floor). For Tests #1 and 2 the anchors were 3/4 in. Grade 5 bolts, while for tests #3, 4, 5 and 6 were 5/8 in. Grade 5 bolts, which passed through holes in the steel plate. These anchors had stiffness similar to post-installed anchors that would be typically used in the field. However, the anchors were designed to remain elastic under the applied loads, since the main objective was to examine the response of the connection controlled by base plate yielding. The top end of the anchors featured a standard hexagonal bolt head (0.8 in., SAE J429 Grade 5), and carbon steel ASTM F844 zinc plated SAE washers for tests #1 and 5 and USS washers for tests #2, 3, 4 and 6. The lower end of these anchors was attached to load cells to enable direct measurement of anchor forces. Referring to Fig. 3b, the load cell is subjected to compression as the anchors are loaded in tension.

**Table 1**
Test and simulation matrix and key results.

| Test/Sim # | Plan layout (See Fig. 4) | Upright | t (in) | $\Delta_{tearing}$ (in) | $\Delta_{tearing}$ Roof Drift | $\Delta_{max}$ (in) | $\Delta_{max}$ Roof Drift | $\frac{F^{FE}_{ref}}{F^{method}_{ref}}$ | $\frac{F^{FE}_{ref}}{F^{current}_{ref}}$ |
|---|---|---|---|---|---|---|---|---|---|
| 1 | A | Channel* | 1/4 | 0.50 | 1.7% | 0.50 | 1.7% | 0.99 | 3.81 |
| 2 | A | Channel | 3/8 | 0.28 | 1.6% | 0.32 | 1.8% | 1.13 | 2.85 |
| 3 | B | Channel | 1/4 | 0.15 | 0.5% | 0.47 | 1.7% | 0.75 | 3.27 |
| 4 | B | Channel | 3/8 | 0.12 | 0.5% | 0.4 | 1.5% | 0.68 | 3.00 |
| 5 | C | Box# | 3/8 | 0.48 | 1.9% | 0.48 | 1.9% | 0.80 | 4.68 |
| 6 | D | Box | 3/8 | 0.12 | 1.0% | 0.44 | 2.4% | 0.37 | 1.95 |
| | | | Mean | 0.28 | 1.2% | 0.44 | 2.0% | 0.79 | 3.26 |
| | | | CoV | 0.63 | 0.52 | 0.15 | 0.17 | 0.33 | 0.28 |

* C4X7.25 welded toe-to-toe.
\# C4X7.25.

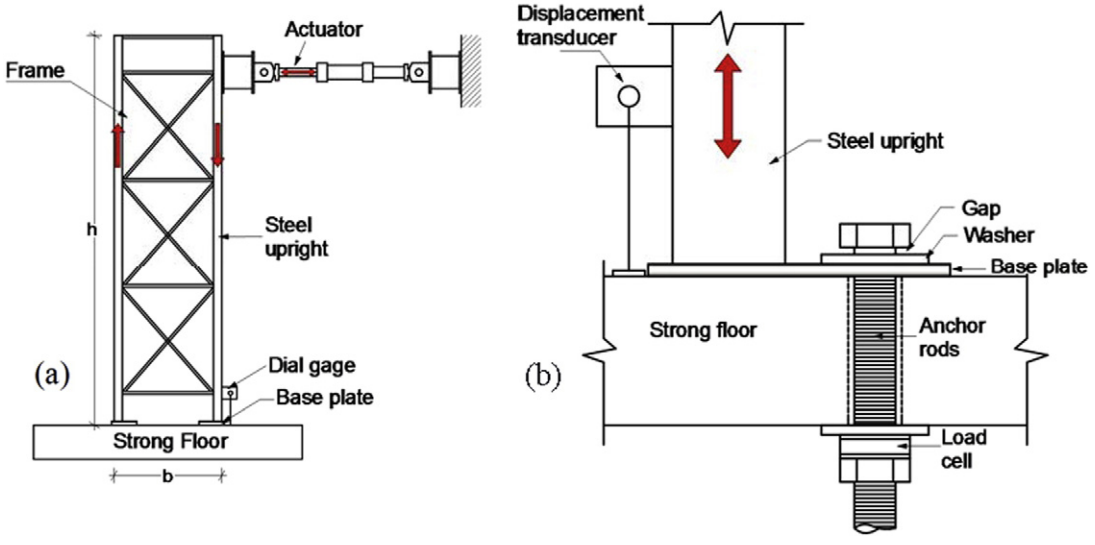


**Fig. 3.** Test setup (a) Overall setup (b) Generic base detail and instrumentation.

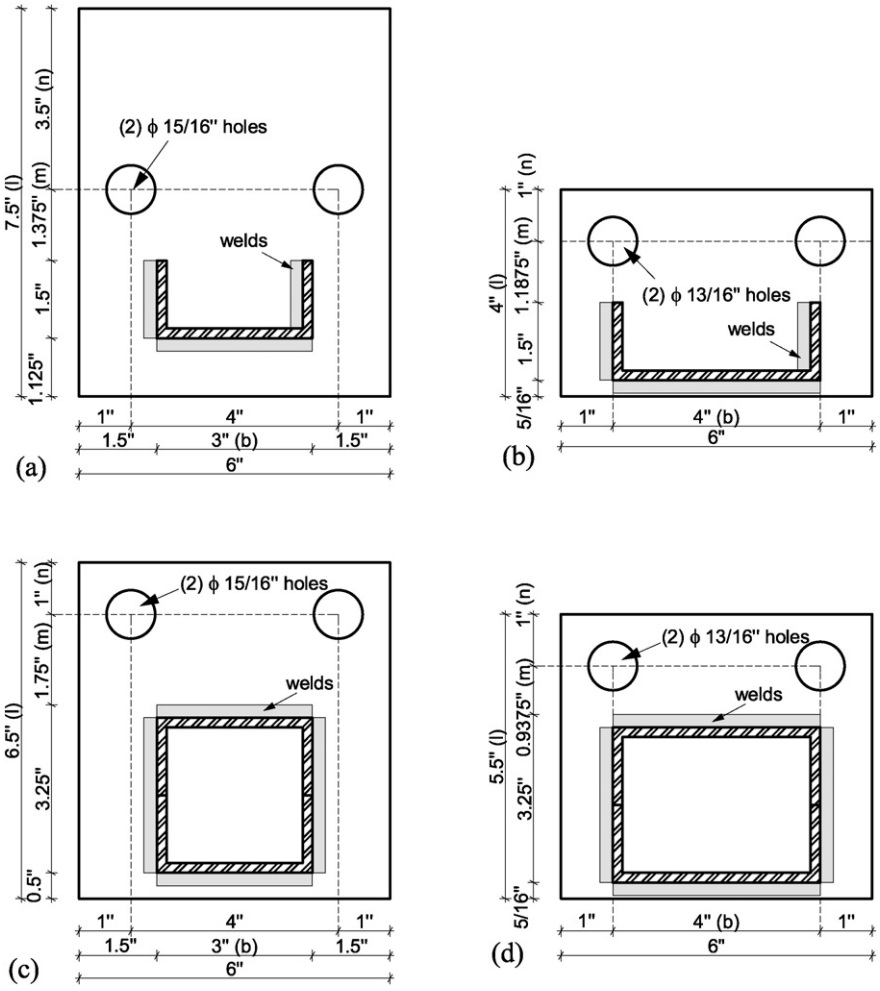


**Fig. 4.** Plan dimensions of the various base plate details; a-d reflect layouts A–D.

5. A small gap (of 0.05 in.) was provided between the washer on the top surface of the plate and the underside of the bolt-head at the top (Fig. 3b) by temporarily placing a shim underneath the top washer. The connection was tightened just enough to still be able to remove the shim by hand prior to starting the test. This gap replicates field conditions for post installed anchor types which exhibit slip under seismic loads (ACI 355 5.5.1.1 and 8.5.3 [21]). This simulates the potential for single curvature bending in the plate at the initial stages of movement. Slip does not occur in all anchor types. However, including it forces the deformations toward the areas where tearing failure initiates, and is therefore conservative for these types.
6. Loads and displacements were measured at the point of application of the lateral load. However, in the context of this study, the measurements in the vicinity of the base connection are equally, if not more, important. These include the anchor forces (discussed above), as well as the vertical displacement of the connection. This was measured using a displacement transducer (see Fig. 3b) attached at a location 6 in. above the base plate.

A direct measurement of the upright force is not possible within this setup. This is because the upright force is not necessarily equal to the sum of the anchor forces because of prying action between the toe of the base plate and the reaction plate. Consequently, the upright force is inferred indirectly through structural analysis of the frame, given the actuator force. Fig. 5a, b, and c show representative force-deformation curves for the base connection (shown here for Test #5). Fig. 5a shows the overall lateral load versus deformation (expressed as

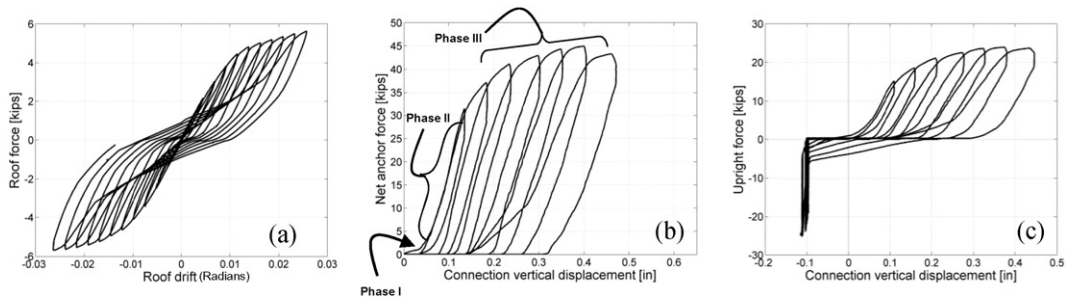


**Fig. 5.** Load deformation curves for (a) Roof force vs lateral displacement (b) Net anchor force vs connection displacement (c) Upright (column) force vs connection displacement.

roof drift) measured at the location of the actuator. Fig. 5b and c focus on the load deformation response of the base connection. In both figures, the plotted displacement is measured by the displacement transducer at the location shown in Fig. 3b. In Fig. 5b, the plotted force is the sum of the forces directly measured in the anchors through the load cells. In Fig. 5c, the force is the estimated upright force; the column force is estimated through structural analysis of the entire frame, based on the applied actuator load. Since inelastic rotation is concentrated only at the base, the force estimated in this manner is consistent with the upright force above the connection. Both these forces are important for different reasons—the measured rod force directly informs design considerations for the post-installed anchors, whereas the upright force-deformation relationship influences the overall design of the frame. Fig. 6a–c show representative photographs of a specimen (for Test #6) at three instants during loading. Referring to Figs. 5a–d, and 6, the following points are noted:

1. Referring to Fig. 5a, the overall load-deformation response of the frame is characterized by an initial elastic slope followed by yielding and pinched hysteresis. As discussed previously, the inelastic response is concentrated entirely in the base connections, which are alternately subjected to tension (uplift) and compression, as the frame is loaded laterally. The pinched hysteresis response may be attributed to the uplift and then *re*-seating of the base plate on the strong floor.
2. Fig. 5b and c show detailed response in the connection region itself. Both these figures show three distinct phases, labeled Phases I, II, and III for clarity. In Phase I, the stiffness is negligible, as the plate lifts vertically without any resistance, owing to the gap above the washer on the top of the plate (see Fig. 3b). Phase II begins when the washer contacts the bolt, and there is a sudden increase in stiffness. This phase is characterized by predominantly elastic response. This continues until base plate starts to yield (Phase III), resulting in a loss in stiffness, and transition to a yield plateau with some degree of hardening. Finally, as the toe of the base plate bends downwards, it contacts the reaction plate (see Fig. 6b). However, an associated increase in resistance is not noticed in the load deformation curve, because the loss in stiffness due to yielding dominates overall response. Two roughly straight yield lines are formed parallel to the web of the upright—one at the edge of the upright, and the other in line with the anchors (see Fig. 6b). The plate bends between these two yield lines in reverse curvature. For convenience, all these phenomena are considered to be a part of Phase III, since they do not show substantive change in the load deformation curve.
3. In specimens except Tests #1 and #5, continued loading results in tearing of the welds between the upright and the plate. This tearing initiates at the extremity of the upright closest to the anchors, and propagates along the sides of the upright cross-section (box or channel) until it reaches the far edge of the upright—see Fig. 6c. In some cases (e.g., Test #6, which features the box section), the fracture extends through the thickness of the plate. It is interesting to note that the load displacement curve does not show a loss of strength despite the initiation and propagation of this fracture. This may be attributed to the following factors: (1) the growth of the crack is gradual, and (2) the loss of strength due to this is compensated for by material hardening, as well as strength increase associated with membrane action, i.e., geometric nonlinearity, as the applied deformations increase.
4. Table 1 summarizes the deformations $\Delta_{tearing}$ (expressed in terms of roof drift as well as the corresponding connection deformation) at which tearing initiates for each of the specimens. It is observed that in some tests, tearing initiates at fairly low levels of deformation (average roof drift of 1.2%). The raises some questions about the seismic performance of these connections, although the tearing does not seem to negatively impact their post-yield response, owing to the compensating factors in the preceding point. In the context of this study, the tearing also complicates the validation of the finite element simulations which are not able to simulate the tearing process directly.
5. The onset of tearing is relatively early in Tests #3, #4, #6; these correspond to the layouts B and D (refer Fig. 4b, d) in which the distance "*m*" between the anchors and the edge of the upright is the least, resulting in highly constrained bending of the plate. On the other hand, the tests with layouts A and C (Tests #1, #2, #5) which have a larger dimension "*m*" appear to show more resistance to tearing. Moreover, for test pairs with the identical layout (Tests #1, #2 with layout A, or Tests #3, #4 with layout B), the thinner (1/4″) plate is more resistant to tearing as compared to the thicker (3/8″) plate. This is not unexpected, given the higher bending strains at the surface of a thicker plate, given similar levels of overall deformation.
6. There was no sudden or brittle fracture observed in any of the 6 tests, with the connection force gradually diminishing until the experiment was terminated due to equipment limitations. Table 1 lists values of deformation $\Delta_{tearing}$ (again expressed as roof drift percentage as well as connection deformation). This is intended to reflect the deformation capacity of the connection, and is determined as the minimum of the peak deformation applied to the specimen and the deformation at which the load drops below 80% of the peak load, following established approaches [22] for such characterization, where the load drop is gradual. When determined in this way, the values of $\Delta_{max}$ are in the range of 1.5%–2.4%, which is significantly higher than the expected demands, which are on the order of 1% as per [6]. When the drifts in Table 1 are interpreted in this context, the experimental results indicate acceptable response for frames within which the base connection (specifically, the plate) is the primary dissipative mechanism. However, it is important to acknowledge that while the load deformation response is acceptable, it is accompanied by significant ductile tearing.

In addition to demonstrating the response of frames with base plate yielding, the experiments support the FE simulations by providing load deformation curves for validation of Finite Element (FE) simulations, which are discussed in the next section.

## 3. Finite element simulation study

The FE simulation study has the following objectives –

1. To provide physical insight into the internal force distribution and deformation modes of the base connection at a level of detail that the experiments cannot, mainly owing to limited and discretely positioned instrumentation.


**Fig. 6.** Photographs at three instants during loading.

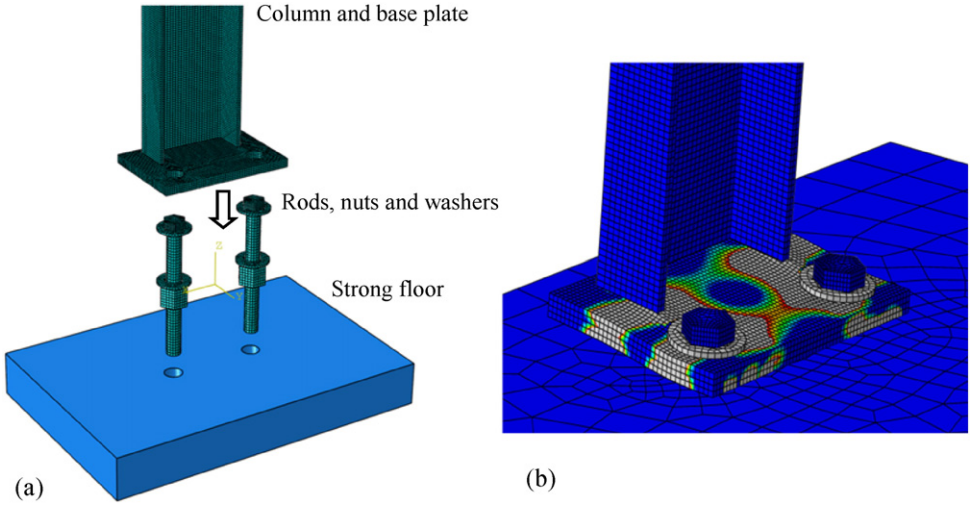


**Fig. 7.** Representative finite element model reflecting Test #4 (a) exploded view (b) plastic strain contours.

2. Once validated, to provide a characterization of baseline connection response without the effects of tearing, based on which analytical models may be developed and validated.

Finite Element models were built complementary to each of the tested specimens, meaning that these models replicated the experiments described previously. Accordingly, the simulations are numbered after the test they complement. A representative FE simulation is shown in Fig. 7. Fig. 7a shows an exploded view of the model, showing the individual parts, whereas Fig. 7b shows a deformed mesh with contours of equivalent plastic strain. This model is complementary to Test #4 (meaning it represents its geometrical and material attributes); other models are similar. The key features of the FE models (constructed using the platform ABAQUS [23]) are:

1. All structural components (upright, plate, anchors, washers, nuts, welds, as well as the reaction plate and load cells) within the models were simulated as discrete parts, which interact as per the relationships illustrated in Table 2. Referring to the Table, the parts may be either "Tied," with the implication that the displacements of their interacting boundaries are constrained, or have frictional contact, implying traction free separation, but the ability to develop bearing and frictional stresses. For all contacts, a friction coefficient of 0.85 was used to represent steel-on-steel response.
2. The FE models included the uprights up to a height of 20 in. above the base plate, since at this height, the stress state in the column was predominantly one of uniaxial stress.
3. The models had between 23,871 and 34,047 elements (depending on geometry), wherein each element was a linear hexahedron solid type element implemented within ABAQUS [23]. The reduced integration provides resistance to volumetric locking of the elements. In the areas of interest in the region of the plate between the column and the anchors (where high stress and strain gradients were anticipated), the mesh was refined, such that the average element dimension was 0.01 in. For each of the specimens, a total of 2 or 4 elements, depending on the actual thickness of the plate, were used to accurately capture bending effects. Fig. 7b illustrates a representative mesh for one of the models (corresponding to Test #4). A mesh sensitivity study confirmed that this degree of mesh refinement was adequate.
4. Constitutive response of the materials (all steel) was simulated through von Mises plasticity with isotropic hardening. The material properties were calibrated from the results of ancillary testing on the materials of the plate, the upright, and the anchors.
5. The reaction plate was restrained at its lower surface, and loading was applied as a vertical displacement to the top surface of the upright stub. Lateral motion of the upright was not restrained. Note that given the aspect ratio of the frame, the motion at the base is predominantly vertical. It is important to emphasize that the simulations were all monotonic. As a result, they capture the backbone response, but cannot simulate processes associated with cyclic loading, such as the pinched hysteresis and degradation. This is considered appropriate within the overall context of the study,

**Table 2**
Interaction properties in FE simulation.

| | Upright | Base plate | Welds | Washer | Rods | Bolts | Nuts | Strong floor |
|---|---|---|---|---|---|---|---|---|
| Upright | – | Tied | Tied | NC* | NC | NC | NC | NC |
| Base plate | Symmetric | – | Tied | Tied | Gap | NC | NC | Contact |
| Welds | | | – | NC | NC | NC | NC | NC |
| Washers | | | | – | Gap | Gap–contact | Tied | Gap |
| Rods | | | | | – | Tied | Tied | Gap |
| Bolts | | | | | | – | NC | NC |
| Nuts | | | | | | | – | Tied |
| Strong floor | | | | | | | | – |

*Not in contact

*not in contact.

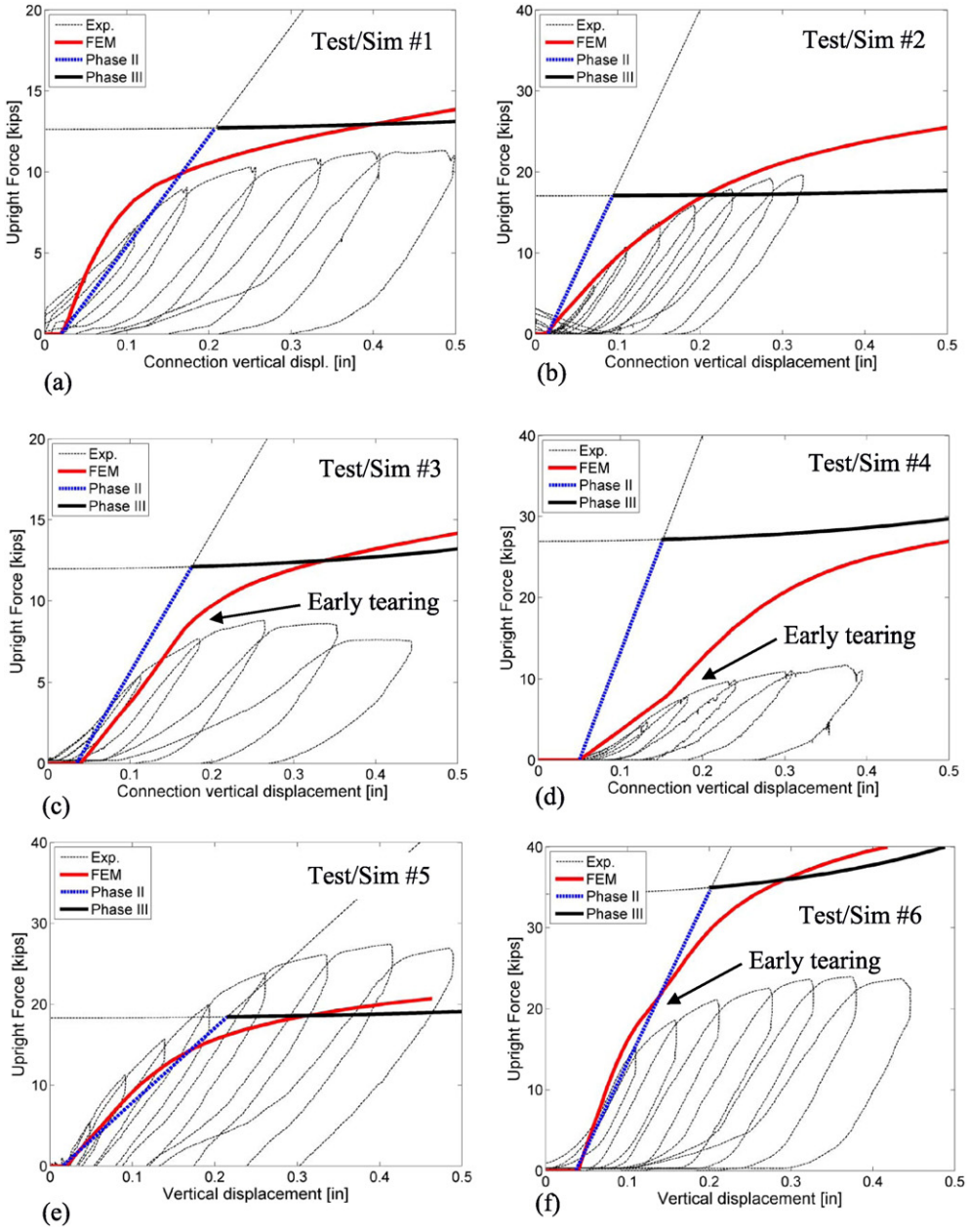


**Fig. 8.** Upright load deformation curves: experimental, finite element model based, and analytical for all experiments and simulations.

whose objectives are to characterize strength and stiffness (i.e., the monotonic backbone) from the perspective of displacement based design.

6. Several quantities and patterns were monitored in the FE simulations. These include: (1) the force in the anchors, and (2) the force in the upright, and (3) the contact force between the toe of the base plate and the reaction plate. In addition, stress, deformation, and yielding patterns were also monitored.

Figs. 8a–f and 9a–f show the load deformation curves for all the 6 simulations overlaid on the experimental load deformation plots for all the simulations. The plots in Fig. 8 represent the upright force plotted against the vertical displacement, whereas those in Fig. 9 are for the anchor forces. The experimental column forces are determined through structural analysis, and are similar to those shown previously in Fig. 5c. The experimental anchor forces are direct measurements (similar to Fig. 5b). In all cases, the experimental displacement is measured at the location indicated in Fig. 3b. The simulation quantities plotted in Figs. 8 and 9 are the counterparts to the corresponding experimental quantities. Also shown on the figures are curves that represent analytical estimates of load-deformation response; this is discussed in a subsequent section. An examination of Figs. 8 and 9 reveals the following points –

1. For 3 of the 6 simulations (except Simulations #1, 2, 5), the monotonic backbone shows reasonable agreement with the experimental envelope for both the upright force as well as the anchor force. In these cases, the deformed shape and yielding patterns predicted by the FE simulations (see Fig. 7), are also strikingly similar to visual observations (see Fig. 6).
2. For the remaining 3 simulations, the load deformation curves are significantly higher than the experimental envelopes. Referring to Table 1, these simulations (i.e., #3, 4 and 6) also show early initiation of weld tearing. As a result, the inaccuracy in the FE simulations is attributed to their inability to simulate crack initiation and propagation in these specimens.

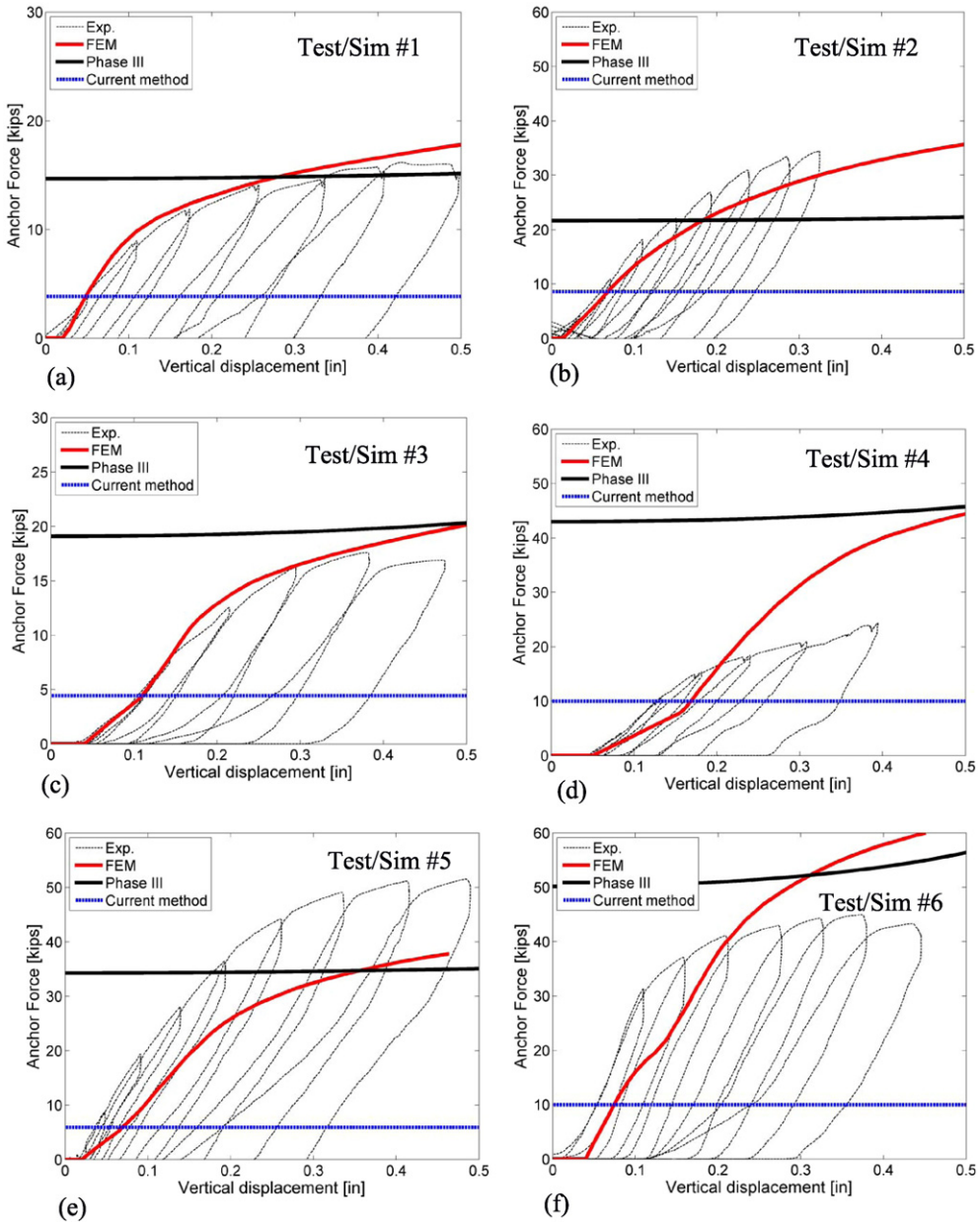


**Fig. 9.** Anchor load deformation curves: experimental, finite element model based, and analytical for all experiments and simulations.

In summary, the FE simulations appear to capture the physical processes controlling connection response (contact, gapping, and yielding) with accuracy as long as weld tearing is inhibited. The implications of this (weld tearing), when developing analytical models for design is discussed in the next section. To further assist in the development of analytical models, deformation and stress patterns in the FE simulations

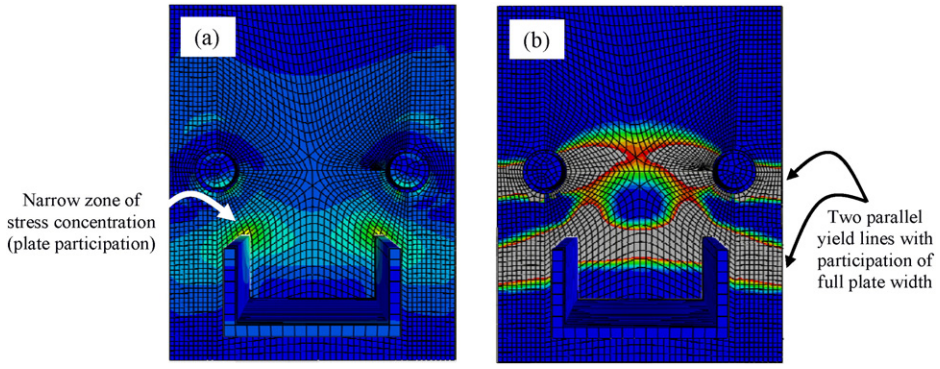


**Fig. 10.** Contours of (a) von Mises stress at low deformation (b) plastic strain at high deformation.

were scrutinized closely. The base plate itself was the primary focus, since connection response was controlled by its yielding. Fig. 10a shows the von Mises stress contours in the base plate (for Test/Sim #1) at a low level of deformation (~0.07 in. after gap closure, i.e., still in the elastic region—refer Fig. 10a). The figure corresponds to the simulation of Test #1. For clarity, the other components (bolt head and washers) are hidden from the view. Referring to the Figure, in the early stages of loading, stress is concentrated in a narrow triangular zone between the anchor rods and the corners of the upright, such that a significant region of the plate does not participate in elastic bending. This may be attributed to two-way bending of the plate, and is consistent with classical plate theory, Timoshenko and Woinowsky-Krieger [24]. Fig. 10b shows plastic strain contours at a larger deformation (~0.35 in. after gap closure, which is on the yield plateau, i.e., Phase III). Referring to this, it is immediately apparent that (1) unlike in the elastic region, the entire width of the plate participates in the yielding mechanism (2) two yield lines (or zones) are formed, and both are relatively straight, and parallel to the web of the column. One of these yield lines is formed near the edge of the upright, whereas the other is formed along the line connecting the anchor rods. In the region between these yield lines, the plate appears to bend in reverse curvature. The increased participation of the plate at higher levels of deformation may be attributed to stress redistribution, which occurs as the regions of the plate (near the anchor rods) first subjected to stress (Fig. 10a) soften leading to incremental stress being transferred to adjacent regions of the plate.

Based on these observations, and the result of the FE simulations, the next section proposes an analytical approach for determining: (1) the load deformation response of the base connections, and (2) the forces in the anchor rods, for which they may be designed.

## 4. Analytical models for backbone response and anchor forces

Building on the FE simulations, this section proposes an analytical approach to characterize base connection response. Specifically, the approach addresses two aspects of response: (1) it provides a method to determine the overall load deformation response of the base connection, i.e., the relationship between the upright force and the connection displacement, and (2) it provides a method to determine the forces developed in the anchor rods as the base plate yields and deforms. The latter is particularly important for design of brittle anchors, which must be able to develop yielding in the base plate.

As noted previously, the overall load deformation response consists of three phases: (I) vertical lifting of the plate with no resistance due to the gap between the bottom of the bolt head and the plate, (II) elastic bending of the plate after it contacts the bolt head, and (III) yielding of the plate. Characterizing the load deformation response over the Phase I is trivial, since it may be assumed to have zero stiffness. The end of Phase I (contact of the plate with the bolt head) is controlled by the size of the gap between the washer and the underside of the bolt head. For post installed anchors used in such construction, this gap is approximately of 0.05 in.; this may be used to inform the analysis.

After the plate contacts the underside of the bolt head, it begins to bend elastically (Phase II). As noted in the previous section and shown in Fig. 10a, due to two way bending, only a small portion of the plate participates in this response. Accordingly, the following expression is presented to characterize load-displacement response in Phase II:

$$F_{II} = \frac{2k_a k_p}{2k_a + k_p}\delta \tag{1}$$

In the above equation $k_a$ is the axial stiffness of the single anchor rod and $k_p$ is the stiffness of the steel plate, while $\delta$ is the vertical displacement of the connection. Specifically, $k_a = E\frac{A_r A_n}{L_r A_n + L_n A_r}$ is calculated accounting for the contribution of both the rod and the bottom nut, where $A$ and $L$ denote the cross-sectional area and length of the rod and the nut, as per the subscript $r$ and $n$, respectively, and $E = 29{,}000$ ksi, is the elastic modulus of steel. Then $k_p = \frac{k_b k_s}{k_b + k_s}$ expresses the overall stiffness of the plate, accounting for both the bending component $k_b = E\frac{l_{eff}t^3}{4m^3}$ and the shear component $k_s = G\frac{5}{6}\cdot\frac{l_{eff}\cdot t}{m}$. In the latter two expressions, $l_{eff}$ represents the plate effective width shown in Fig. 11, $t$ is the thickness of the plate, $m$ is the distance between the anchor rod centroid and the closest tips of the weld, and $G = 11.150$ ksi, is the shear modulus of steel. It is immediately evident that Eq. (1) represents a linear response, with constant stiffness $\frac{2k_a k_p}{2k_a + k_p}$. The stiffness reflects contribution from the base plate and the anchor rods acting in series (such that their deformations are additive). The base plate stiffness is controlled by the bending of two "cantilever strips" of the plate, shown in Fig. 11. Referring to the figure, the width of these cantilever strips (equaling the total effective width of the plate $l_{eff}$) is determined by constructing a 30-degree influence cone around the line representing the shortest distance between the center of the anchors and the upright. This construction represents the extent of participation of the plate, as observed in the FE simulations (see Fig. 10a).

Eq. (1) also includes the contribution of shear deformations, as well as the elongation of the anchor rods. The efficacy of this approach to characterize Phase I response is discussed later in this section. As discussed previously, Phase III is associated with post-yield response of the base plate. This regime is characterized by several interacting phenomena: (1) redistribution of stresses to engage a larger width of the base plate in yielding, (2) contact of the plate toe with the reaction plate to produce reverse curvature bending of the plate and an associated yield line along the anchors, and (3) stiffening of the

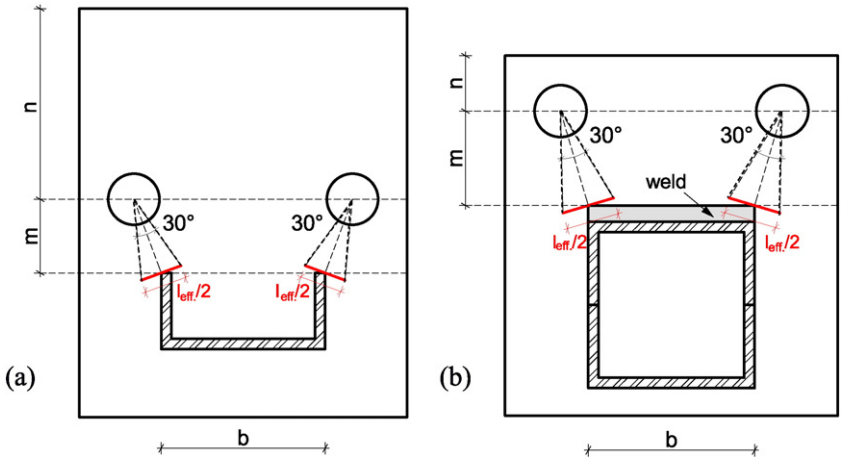


**Fig. 11.** Model assumptions for calculating elastic stiffness (Phase II response) shown for (a) Channel upright (b) Box upright.

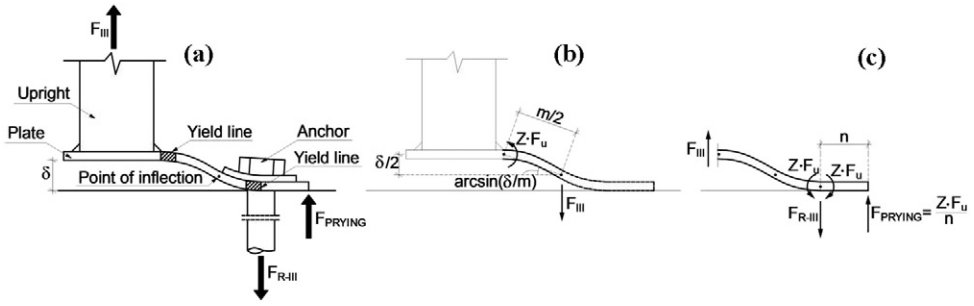


**Fig. 12.** Model assumptions for calculating post-yield (Phase III) response.

plate with increasing deformations, due to membrane action (change in angle as the vertical displacement increases relative to the horizontal span of the plate). Referring to prior discussion, the effect of contact (which increases the stiffness) cannot be isolated from that of yielding (which reduces stiffness), such that overall stiffness of the base connection does not show a measurable increase in stiffness as contact occurs. Neither the initiation of contact, nor the redistribution of stresses (through the width) is explicitly considered in the analytical model for Phase III. Instead, Phase III response is described through a mechanism-based limit analysis, which is schematically illustrated in Fig. 12.

Referring to Fig. 12a, the mechanism consists of the base plate rotating between two fully formed yield lines, one at the edge of the column and the other in line with the anchors. Furthermore, it is assumed that each of the yield lines carries a moment $M_{plate} = Z \cdot F_u$, where $Z = \frac{bt^2}{4}$ is the plastic section modulus and $F_u$ is the ultimate stress of the base plate steel. Both these assumptions are based on: (1) stress and deformation patterns recovered from the FE simulations, and (2) agreement with experimental and FE-based load deformation curves. It is important to note that the plate moment strength $M_{plate}$ is determined using the ultimate strength $F_u$, instead of the yield stress $F_y$. This is because (as indicated by FE and corroborated by agreement with experimental data) significant strain hardening occurs in the plate. Also, while $F_y$ may be used for design of the base plate (Fisher and Kloiber [25]), it is not appropriate where the strength of the base plate controls the capacity design of adjoining brittle anchors. Here the anchors must be designed for the maximum deliverable force. However, where the maximum deliverable force exceeds 2 times the anticipated demand, the system overstrength governs. Eq. (2) expresses a relationship between the upright displacement and force, based on the yield line pattern shown in Fig. 10b, and the deformation profile shown in Fig. 12b.

$$F_{III} = F_u \cdot Z \cdot \frac{1}{{}^1/_2 \cdot m \cos\left(\arcsin\left(\frac{\delta}{m}\right)\right)} \tag{2}$$

Referring to Eq. (2) above, and Fig. 12b, the plate is assumed to have a point (line) of inflection midway between the centerline of the anchor rods and the edge of the columns—this results in the factor ½ in the denominator of Eq. (1) above. Alternative locations for the yield lines, as well as other yield line patterns were examined, but they did not provide sufficient improvement in model accuracy to justify their complexity. The ${}^1/_2 \cdot m \cos(\arcsin(\frac{\delta}{m}))$ term in the denominator of the Equation represents the stiffening due to membrane action, as the plate rotates. Eq. (3) below is similar to Eq. (2), except that it represents a relationship between the anchor force (instead of the upright force) and the column displacement –

$$F_{R-III} = F_u \cdot Z \cdot \left(\frac{1}{{}^1/_2 \cdot m \cos\left(\arcsin\left(\frac{\delta}{m}\right)\right)} + \frac{1}{n}\right) \tag{3}$$

Referring to the equation above, the anchor force reflects an additional term corresponding to the prying force, which arises from bending of the plate toe in the region between the anchors and the edge of the plate (see Fig. 12c). As a result, the net force in the anchors may be considered the sum of the upright force and the prying force, which is determined as the plastic moment carried in the yield line, divided by an appropriate lever arm distance. Based on the FE simulations and experimental results, this distance is determined to be the distance between the centerline of the anchor rods, and the edge of the plate. Note that the yield line at the location of the anchor is assumed to be wide enough to subsume the width of the anchors, such that the plastic moment is present on both sides of the anchor centerline.

In summary, while Phase I has zero stiffness, Phases II and III of response may be generated from Eqs. (1) and (2). This results in a piecewise function describing the response of the base connection. Piecewise functions generated in this manner are overlaid on the experimental and simulation plots for all the tests in Fig. 8a–f (for the upright load displacement, i.e., Eqs. (1) and (2)) and in Fig. 9a–f (for the anchor rod load displacement, i.e., Eq. (3)). Note that Fig. 9a–f do not contain two analytical curves (Phase I response is not shown), since the elastic loading portion is not relevant for anchor design. Before comparing the analytical curves to the experimental/FE curves, it is useful to recall that neither the FE simulations, nor the analytical equations consider the effect of tearing, which is present in some of the test specimens. As a result, the efficacy of the analytical method is evaluated relative to the FE simulations, rather than the experiments, acknowledging that the method cannot simulate tearing. The implication is that the method may be applied with confidence to configurations where tearing is mitigated. The design implications of the tearing itself are discussed in the next section. A review of Fig. 8a-f reveals the following observations –

1. By and large, the analytical approach with the piecewise curve provides a reasonable envelope for the FE-based load deformation curves, and for the experimental curves, in Tests #1, #2, and #5 where tearing is delayed.
2. The analytical approach provides a better agreement overall for Phase III response (i.e., the post-yield, where on average, the analytical curve is within 20% of the FE yield plateau), than it does for the elastic stiffness (Phase II). The agreement for the elastic stiffness is less satisfactory for simulations #2, #4, which feature the box column, and the thicker plate (i.e., 3/8 in.).
3. The agreement in the transition region between Phase II and Phase III is weak for all the simulations. This is because the analytical curves (described by (1) and (2)) do not consider this transition. As discussed previously, the transition from the initial elastic response to the final plastic limit state is characterized by redistribution of stresses from the narrow width near the corners of the column (Fig. 10a) to full engagement of the base plate width (Fig. 10b). The analytical curves reflect only the initial and final stages of this transition, and consequently do not capture the gradual loss of stiffness associated with it. The implications of this may be considered

modest where the load-deformation curve is used in the context of deformation-based design methods, such as the capacity spectrum method [26], or the Direct Displacement Based Design (DDBD) method [27]. This is because these methods rely on the response (base shear or secant stiffness) in the vicinity of the design or limit displacement. This displacement is typically associated with significant ductility, and is located on the yield plateau—a region in which the analytical method shows good accuracy.

Fig. 9a–f show net force in the anchor rods plotted against connection deformation. The figures also show the analytical estimate of the anchor force as determined through Eq. (3). For additional reference, the figures also show the anchor force determined as per Eq. (4) below

$$F_{R-curr} = F_y \frac{Z}{m} = F_y \frac{bt^2}{4}\frac{1}{m} \tag{4}$$

The above equation represents the prevalent approach for anchor design, which disregards the material hardening (it is based on the yield stress), the membrane action, and also assumes that the plate bends in single curvature, thereby disregarding prying forces. As a result, it significantly underestimates the anchor forces, which is unconservative and concerning, since post installed anchors are brittle. On the other hand, the anchor forces determined by the proposed method consider all these effects. Consequently, the estimated forces are significantly greater. However, since both the FE and the analytical curves are displacement dependent, it is somewhat challenging to uniquely quantify the accuracy of the analytical method with respect to the FE curves. To overcome this, it is useful to evaluate the analytical method within the context in which it may be ultimately applied for design. From a behavioral standpoint, the anchors must be designed to resist the forces that are developed in the vicinity of the design displacement. Following prior literature [6] and professional judgment, the frames typically undergo a peak roof drift of 1%. For each of the frame specimens, the associated connection deformation is determined from the experimental measurements. The forces ($F_{ref}$) at this reference deformation (which is indicative of the expected performance point) may be compared between the analytical and FE models to assess the analytical model. For example, for any simulation, the ratio $F_{ref}^{FE}/F_{ref}^{current}$ reflects the ratio between the anchor force determined from the FE simulations, to the anchor force determined as per the current design method, i.e., Eq. (4). Referring to Table 1, the average value of $F_{ref}^{FE}/F_{ref}^{current}$ is 3.26 with a Coefficient of Variation (CoV) = 0.28. This indicates that current method grossly underestimates the forces in the anchors, and is highly unconservative. This is not surprising because the method disregards key aspects of response including strain hardening, membrane action and the plate fixity at the anchor rods, which results in double curvature bending. This finding corroborates previous experimental results [28], which indicate a similarly high strength associated with plate bending. While not surprising, this finding is disconcerting, since it suggests that the current approach may result in unconservative design of the brittle anchors. Table 1 also summarizes the ratios $F_{ref}^{FE}/F_{ref}^{method}$, wherein the denominator is determined as per the proposed method, i.e., Eqs. (1)–(2), which incorporate the various effects disregarded by the current approach. Referring to the Table 1, the average value of $F_{ref}^{FE}/F_{ref}^{method}$ is 0.79, with a Coefficient of Variation 0.33. This indicates that the proposed method provides good agreement with the simulated forces in the anchors, implying a vast improvement for the safe design of anchors. The next section discusses the design implications of the experimental and simulation program, as well as the proposed analytical models.

## 5. Summary, implications for design, and limitations

The study examined the response of column base connections in storage racks subjected to cross-aisle lateral loading. In this direction, the racks are composed of braced frames, whose mode of inelastic dissipation is not clearly defined. Prior experimental investigations reveal non-ductile deformation modes adjacent to the bracing connections, whereas the current design practice for these frames uses a force based method, with *R*-factors that are not based on rigorous analysis of the structural system. Motivated by this, the primary objective of the study is to examine the feasibility of a dissipative mechanism that relies on base connection yielding during cross aisle response of the storage racks, and then to provide design support for this system.

The main scientific basis of this study is a set of 6 full-scale experiments on braced frames that represent storage rack frames loaded in the cross aisle direction. In the experimental program, all frames were loaded laterally at the top, and designed to concentrate yielding in the base connections. The main variables investigated were the base plate thickness and layout, and the upright cross section (channel or box). The base connections themselves were designed to yield through flexure of the base plate, such that the anchors remained elastic. This is consistent with the intended response wherein the brittle post-installed anchors are expected to remain elastic as the base plate yields. The connections were specially instrumented with load cells to directly measure the anchor forces. Complementary Finite Element (FE) simulations were conducted for each of the experiments. The objective of the FE simulations was to provide quantitative insights into the internal stress and deformation patterns in the connections, to inform analytical equations for connection response and design.

The main observation from the experiments is that base yielding appears to be a feasible dissipative mechanism for seismic design of storage racks in the cross-aisle direction. The load deformation response of the base connection has a stable yield plateau, without significant strength loss well beyond the expected deformation demands. Ductile tearing is visually observed at the weld between the upright and the base plate. In specimens with the thicker plates and a short distance between the anchors and upright, the ductile tearing initiates fairly early, whereas it is delayed in the specimens with the thinner plates and a greater distance between the anchors and the column. However, the tearing is gradual and does not result in a loss or degradation of strength. As a result, the component behavior in itself may be considered adequate, in the sense that it shows an acceptable load-deformation response. Nonetheless, the tearing observed in some of the specimens is significant since the associated ductility may not be generalizable to materials (toughness properties) and configurations that are dissimilar to the ones tested in this study. Assuming that the tearing may be mitigated (through the use of thinner base plates or alternate configurations) or tolerated, the design requires two additional considerations:

1. The load-deformation response of the base connection must be generalized, such that it may be used within a displacement based design framework [27], or as a "backbone curve" for a cyclic component model to be used within a comprehensive simulation program for *R*-factor calibration [12]. Analytical equations are developed to characterize the load-deformation response. These equations are based on an assumed deformation modes and yield line patterns that are informed by the experimental data (quantitative and visual observations), and the FE simulations. The analytical equations are able to capture the initial elastic response, and the yield plateau with reasonable accuracy. However, they cannot capture the transition between these two phases of behavior, which is controlled by distribution of yielding through the width of the base plate.
2. To achieve the response discussed above, the base connection must be detailed to deform in a ductile manner. To ensure this, two potential brittle modes must be mitigated. The first is fracture of the plate, or the weld between the upright and the weld. Additional work is needed to fully establish details that do not result in this fracture, although the experiments suggest that the use of channel uprights and thinner (1/4″) base plate with a larger distance between the

anchors and the upright delays the onset of tearing. However, it is noted again that even with the visually observed tearing, the load-deformation response of the tested connections may be considered acceptable. The second potential brittle mode is the pullout of the post-installed anchors. To mitigate this, the anchors must be designed for tensile forces that can develop yielding and strain hardening in the base plate at deformations consistent with anticipated demands. The current method for designing these anchors assumes single curvature bending of the base plate, and does not consider the effect of strain hardening or membrane action—both of which increase the force in the anchors. As a result, the method is grossly unconservative. A new approach is presented to characterize anchor forces—this method compares favorably with the simulated forces in the anchors, because it incorporates the phenomena disregarded by the currently used method.

In summary, the study demonstrates the base-yielding mechanism for storage racks subjected to seismic loading in the cross-aisle direction. The complementary FE simulation and analytical development provide support for design of the frames and the connection itself. However, the study has limitations which must be considered in the interpretation of its results and the application of the methods that arise from it. From a behavioral standpoint, the ductile tearing is a concern, and future work may be directed at (1) interrogating base plate configurations that effectively mitigate it, or (2) establishing that the acceptable load-deformation response observed along with the ductile tearing (as in this study) is general across different configurations, weld details, and material types. From a methodological standpoint, some issues need to be noted. First, the experimental program is relatively modest in scope, and care must be taken in extrapolating the findings to configurations significantly dissimilar to those tested. Second, the study characterizes the capacity of these components, and assesses it relative to the demands. However, the demands themselves are determined from other studies on similar frames. Third, this study considers the response of base connections in the cross-aisle direction only. However, these connections are likely subjected to biaxial loading. More specifically, during seismic shaking, the connections are subjected to rotational deformations in the down-aisle direction (due to moment frame action), along with vertical deformation in the cross-aisle direction as examined in this study. Finally, the FE simulations and the analytical models do not explicitly consider cyclic loading, and thus can only simulate the backbone or envelope, and not the hysteretic response. It is acknowledged that these issues are outside the scope of the current study, and a resolution of all these issues warrants further testing, simulation, and design and methodological development (e.g., as outlined in [29]) which is ongoing as of this writing.

## Acknowledgments

The authors gratefully acknowledge the Frazier Industrial Company for providing the experimental specimens, setup and technical support, particularly Phil Hathaway and Wen Shan. The opinions and findings in this paper are those of the authors and may not reflect those of the sponsors.

## References

[1] Federal Emergency Management Agency FEMA, Seismic Considerations for Steel Storage Racks Located in Areas Accessible to the Public, FEMA460, Washington, D.C. 2005.
[2] H. Krawinkler, N.G. Cofie, M.A. Astiz, C.A. Kircher, Experimental Study on the Seismic Behavior of Industrial Storage Racks, Report No. 41, The John A. Blume Earthquake Engineering Center, Stanford University, Stanford, CA, 1979.
[3] P. Higgins, Personal Communication, Peter Higgins and Associates, Malibu, CA, 2004.
[4] C. Bernuzzi, C.A. Castiglioni, Experimental analysis on the cyclic behavior of beam-to-column joints in steel storage pallet racks, Thin-Walled Struct. 39 (2001) 841–859.
[5] John A. Blume & Associates, Seismic Investigation of Steel Industrial Storage Racks, Report Prepared for the Rack Manufacturer's Institute, San Francisco, CA, 1973 (43 pp.).
[6] C.K. Chen, R.E. Scholl, J.A. Blume, Earthquake Simulation Tests of Industrial Steel Storage Racks, Proceedings of the Seventh World Conference on Earthquake Engineering, Istanbul, Turkey 1980, pp. 379–386.
[7] C.A. Castiglioni, N. Panzeri, J. Brescianini, P. Carydis, Shaking Table Tests of Steel Pallet Racks, Proceedings of the Conference on Behaviour of Steel Structures in Seismic Areas-Stessa 2003, Naples, Italy 2003, pp. 775–781.
[8] A. Filiatrault, P. Higgins, Shake Table Tests of Storage Racks and Contents, Presentation material at the April 12, 2000 Seismic Safety Commission Hearing on Industrial Storage Racks, San Francisco, CA, 2001.
[9] A. Filiatrault, A. Wanitkorkul, Shake-Table Testing of Frazier Industrial Storage Racks, Report no. CSEE-SEESL-2005-02, Structural Engineering and Earthquake Simulation Laboratory, Departmental of Civil, Structural and Environmental Engineering, University at Buffalo, State University of New York, 2004 (83 Pp.).
[10] G.E.N.R. Coutinho, Numerical Simulation of the Seismic Behavior of Steel Storage Pallet Racking Systems(Master dissertation) Technical University of Lisbon, Portugal, 2008.
[11] C.K. Chen, R.E. Scholl, J.A. Blume, Seismic Study of Industrial Storage Racks, Report Prepared for the National Science Foundation and for the Rack Manufacturers Institute and Automated Storage and Retrieval Systems (Sections of the Material Handling Institute), URS/John A. Blume & Associates, San Francisco, CA, 1980 (569 pp.).
[12] International Conference of Building Officials, Uniform Building Code, ICBO, Whittier, CA, 1975.
[13] Rack Manufacturers Institute, Specification for the Design, Testing and Utilization of Industrial Steel Storage Racks, ANSI MH16.1:2012, RMI, Charlotte, NC, 2012.
[14] American Society of Civil Engineers, Minimum Design Loads for Buildings and Other Structures, ASCE/SEI 7–10, Reston, VA, 2010.
[15] M. Midorikawa, T. Ishihara, T. Azuhata, H. Hori, T. Kusakari, T. Asari, Three-Dimensional Shaking Table Tests on Seismic Response of Reduced-Scale Steel Rocking Frames, 3rd International Conference on Advances in Experimental Structural Engineering, San Francisco, 2009.
[16] A.A. Huckleridge, Earthquake simulation tests of a nine storey steel frame with columns allowed to uplift, EERC-77/23, University of California, Berkeley, CA, 1977.
[17] X. Ma, G. Deierlein, M. Eatherton, H. Krawinkler, J. Hajjar, T. Takeuchi, K. Kasai, M. Midorikawa, T. Hikino, Large-Scale Shaking Table Test of Steel Braced Frame with Controlled Rocking and Energy Dissipating Fuses, Proceedings of the 10th US National and 10th Canadian Conference on Earthquake Engineering, Toronto, Canada, 2010.
[18] S. Acikgoz, A. Argyle, M. Dejong, The Role of Supplemental Damping in Limiting Forces and Displacements in a Rocking Structure, Second European Conference on Earthquake Engineering and Seismology, Istanbul, Turkey, 2014.
[19] M. Gesoglu, T. Ozturan, M. Ozel, E. Guneyisi, Tensile behavior of post-installed anchors in plain and steel fiber-reinforced normal- and high-strength concretes, ACI Struct. J. 102 (2) (2005) 224–231.
[20] ATC-24, Guidelines for Cyclic Seismic Testing of Components of Steel Structures for Buildings, Report No. ATC-24, Applied Technology Council, Redwood City, CA, 1992.
[21] ACI Committee 355.3R., Guide for Design of Anchorage to Concrete: Examples Using ACI 318 Appendix D, American Concrete Institute, Farmington Hills, MI, 2011.
[22] Federal Emergency Management Agency FEMA, Recommended Seismic Design Criteria for New Steel Moment-Frame Buildings, FEMA350, Department of Homeland Security, Washington, D.C., 2000
[23] ABAQUS, ABAQUS/CAE 6.14–1, Dassault Systèmes, 2014.
[24] S. Timoshenko, S. Woinowsky-Krieger, Theory of Plates and Shells, second ed. McGraw-Hill book company, 1989.
[25] J.M. Fisher, L.A. Kloiber, Base Plate and Anchor Rod Design, Steel Design Guide Series No. 1, second ed.American Institute of Steel Construction, Inc., Chicago, IL, 2006.
[26] S.A. Freeman, Review of the Development of the Capacity Spectrum Method, ISET Journal of Earthquake Technology, Paper No. 438, vol. 41, No. 1 2004, pp. 1–13.
[27] M.J.N. Priestley, G.M. Calvi, M.J. Kowalsky, Direct Displacement-Based Seismic Design of Structures, New Zealand Society for Earthquake Engineering Inc., 2007 (NZSEE Conference).
[28] A.M. Kanvinde, P. Higgins, R.J. Cooke, J. Perez, J. Higgins, Column base connections for hollow steel sections: seismic performance and strength models, J. Struct. Eng. ASCE (2014), http://dx.doi.org/10.1061/(ASCE)ST.1943-541X.0001136.
[29] C. Faella, V. Piluso, G. Rizzano, Structural Steel Semirigid Connections: Theory, Design, and Software, CRC Press, 1999.